

IFSCC 2025 full paper (**IFSCC2025-1508**)

“Based on network pharmacology and molecular docking to explore the anti-aging and anti-inflammatory mechanism of Terminalia Chebula extract at AKT1 target”

Zhihua Zhang¹, Yimeng Wang¹, Huihui Zhang¹, Can Huang², Ji Zhou², Zhanlin Ma², Tao Zhang¹,

¹ Department and Development Center, Better Way (Shanghai) Cosmetics Co.Ltd.

² Ingredi Biotech Co., Ltd.

1. Introduction

The occurrence of sensitive skin is a complex process involving skin barrier, neurovascular response, innate immune inflammation. In the meanwhile, there is lack of comprehensive study on sensitive skin aging with unclear potential pathways. We used network pharmacology and molecular docking to find these potential gene targets: AKT1 and then verified them through efficacy experiments and clinical trials, and found that Terminalia Chebula is a novel effective raw material for the treatment of sensitive skin aging through AKT1 pathway. The gene target of Terminalia Chebula extract (TCE) in the skin was studied by network pharmacology and molecular docking, and the target pathway of AKT1 was locked. The model established by AKT1 on macrophages was validated through experiments, and the effects of NRF2, TRPV1 ,TNF- α and other inflammatory factors were verified. The main chemical components of TCE were detected and analyzed by high performance liquid. Its immediate and long-lasting soothing and anti-aging effects have been verified in humans.

2. Materials and Methods

2.1. Chemicals and reagents

Terminalia Chebula extract (TCE) was obtained from the Ingredi Biotech Co., Ltd.

Gallic acid, Chebulagic acid ,Chebulinic acid was obtained from the Shanghai Yuanye Bio-Technology Co., Ltd.

LPS and VE were obtained from the Sigma-Aldrich, Resveratrol (C16677387) was obtained from the Macklin. PP1 inhibitor (012224240607) was obtained from the Beyotime. Akt1 (C73H10) Rabbit mAb (C2938T) , Phospho-Akt1 (Ser473) (D7F10) XP® Rabbit mAb (9018T) , β -Actin Antibody (4967L) , Anti-rabbit IgG, HRP linked Antibody (7074P2) was obtained from the CST. Reverse Transcription Kit: PrimeScript™ RT Reagent Kit (Perfect Real Time) (RR037A) was from TaKaRa, qPCR Detection Kit was from Hery Bio.. Capsaicin , Capsazepine and Dexamethasone were obtained from the MedChemExpress. Nrf2 antibody was obtained from the Abcam. High-performance liquid chromatography (HPLC)-grade acetonitrile and methanol were purchased from Aladdin Biochemical Technology Co., Ltd. (Shanghai, China). High purity deionized water (18.2 MΩ·cm) was generated using an Arium® Comfort I water purification system (Sartorius AG, Göttingen, Germany). The

analytical grade phosphoric acid was obtained from the Tianjin Fuyu Fine Chemical Co., Ltd.. Human skin fibroblast cells HSF (BNCC341540) and mouse monocyte-macrophage leukemia cells RAW 264.7 (BNCC354753) and Hacat cell were obtained from the BNCC.

2.2 HPLC analysis of TCE

The chromatography analysis was performed using an Agilent 1260 Infinity II HPLC system (Agilent Technologies, CA, USA) equipped with a diode array detector (DAD) and a reversedphase C18 column (250 × 4.60 mm, 5 µm) (Agilent Technologies, CA, USA). The gradient elution program employed mobile phase A (0.1% phosphoric acid) and B (Methanol) under the following conditions: 0–10 min, 1.5–5% B; 10–30 min, 5%–50% B; 30–35 min, 50%–2% B, with a constant flow rate of 1.0 mL/min. The column temperature was maintained at 35°C with a 10-µL injection volume. The DAD detection spanned 200 to 600 nm, with quantitative integration performed at 273 nm. Chromatograms as well as absorption spectra in the UV were obtained for each component using HPLC. TCE samples were prepared in 1 mg/mL to test [1-2].

2.3 Network pharmacology and molecular docking of

Screening of TCE and target prediction of TCE active compounds : The smile format of small molecule gallic acid, chebulagic acid and chebulinic acid was obtained from pubchem and imported into Swiss Target Prediction to predict targets. Subsequently, the predicted targets and the aging and inflammation-related targets in the own database were intersected respectively. The string database was used to analyze protein-protein interaction (PPI) network analysis of intersection targets. Cytoscape was used for core target screening^[3-4].

Enrichment analysis of biological processes and pathways : The potential targets of TCE active components related to aging and inflammation were put into the Metascape platform. After submission, select both the input species and the analyzed species as "H.sapiens", set P<0.01, conduct Gene Ontology (GO) annotation analysis and Kyoto Encyclopaedia of Genes and Genomes (KEGG) pathway analysis on the targets of TCE action, and save the results. And sort them according to the number of targets involved in each item, and screen out the GO functions and pathways with higher rankings. The data of the potential targets and metabolic pathways of the active components of TCE were imported into the Cytoscape3.5.1 software, and the "component - target - pathway" network model of TCE AKT1 was constructed using the Merge tool.

Molecular docking verification: Discovery Studio software was used for docking. The 3D structure of the small molecule ligand was obtained from the pubchem and the energy minimization was performed in the Discovery Studio software. The crystal structure of AKT1 (PDB ID: 4EJN.pdb) was gained from the PDB database. Remove excess water and cofactors contained in protein crystals, and perform hydrogenation procedures according to docking requirements. A docking sphere with a radius of 25 Å was constructed, and its active center coordinates were x = 27.031552, y = 58.807761, z = 4.691362. Docking was performed using "CDOCKER" under the "Docking Optimization" module, and "-CDOCKER ENERGY" was used to evaluate the direct interaction between the ligand and the receptor.

The crystal structure of AKT1 (PDB ID: 4EJN.pdb) was gained from the PDB database. The 2D structures of gallic acid, chebulin tannic acid and chebulin tannic acid.sdf files were obtained from pubchem. Subsequently, the AKT1 and small molecule.sdf files were imported into CB-Dock2 respectively, and the "Auto Blind Docking" mode was selected for docking. The "Structure-based Blind Docking" was selected to obtain the ligand-receptor docking complex for analyzing the interaction force. Pymol software was used to analyze and visualize the molecular docking results^[5-7].

2.4 Akt1 target validation

The human skin fibroblasts were stimulated with UVA (5 Jcm^2 , perpendicular to the cell plate, UVA away from the cell plate 4cm, irradiation intensity $1400\mu\text{W}/\text{cm}^2$) for 60 minutes. Then, sample solutions of different concentrations were added. Meanwhile, a blank group, a model group, and a positive control group (Resveratrol) were set up, and the action was carried out for 48 hours. After the action time ended, the cells were lysed for protein expression testing. Mouse mononuclear macrophage leukemia cells were first stimulated with LPS ($5\mu\text{g}/\text{mL}$) for 24 hours. Then, sample solutions of different concentrations were added. Meanwhile, blank groups, model groups and positive control(PP1 inhibitor) groups were set up and acted for 24 hours. After the action time ended, the cells were lysed for protein expression testing^[8] Whole protein extraction, membrane protein extraction, nuclear protein extraction were aliquot and store in a refrigerator at -80° C .

Protein electrophoresis and membrane transfer: Place the electrophoresis tank in an ice bath and perform electrophoresis at a voltage of 70 V for 30 minutes to compress the loaded protein sample into a narrow line. Then, change the voltage to 120 V for electrophoresis until the blue bromophenol blue reaches the bottom of the gel, which takes approximately 90 minutes. According to the principle of "black glue white surface", place the PVDF membrane in the transfer clamp and use a rapid transfer instrument for protein transfer^[9-10].

2.5 Effects of TCE on Nrf2

3D epidermal skin model (Epiutis®, ES240604), was obtained from the Biocell Co. , Ltd.

Transfer the 3D epidermal skin model to a 6-well plate and mark the test group number on the 6-well plate. In blank groups and Negative Control groups, 0.9mL of model culture medium was added to each well, while in positive control group, 0.9mL of model culture medium containing VE was added to each well. The sample group was administered by surface administration, with a dosing volume of $25 \mu\text{L}$ per model. During administration, it was spread evenly with a gentle tap to ensure full absorption of the sample. After the administration was completed, all groups except the blank control group underwent UVB irradiation, with an irradiation dose of $600\text{mJ}/\text{cm}^2$.

After irradiation, the 6-well plate was incubated in a CO_2 incubator (37° C , $5\% \text{CO}_2$) for 24 hours. The model was cleaned and then fixed. After being fixed for 24 hours, immunofluorescence detection was carried out. Photos were taken under a microscope for observation, and the pictures were collected and analyzed^[11].

2.6 Effects of TCE on TRPV1

After the Hacat cells were grouped and administered, model groups ($10 \mu\text{L}$ capsaicin) and positive control groups ($10 \mu\text{L}$ Capsazepine) were set up. The sample solutions of different concentrations were added in the sample groups. The culture ended after 24 hours, and the supernatant was collected for ELISA detection. Inhibition rate (%)=(1- Sample group/model group)*100% ^[12].

2.7 Effects of TCE on TNF- α

After the RAW264.7 cells were grouped and administered, model groups ($1 \mu\text{g}/\text{mL}$ LPS) and positive control groups ($10 \mu\text{L}$ Dexamethasone) were set up. The sample solutions of different concentrations were added in the sample groups. The culture ended after 24 hours, and the supernatant was collected for ELISA detection ^[13-15].

2.8 Cell viability assay

Effect of Terminalia Chebula (0e10 mM) on the viability of RAW264.7 and HSF cells and Hacat cell for 24 h was evaluated by an MTT assay as previously reported .

2.9 Clinical study

Results were collected by VISCR in 30 subjects (36-60 years old) with sensitive skin using the cream (0.3% TCE-containing essence cream) of this test sample for 7 consecutive days. Subject information registration, completion of understanding and signing of the informed consent form, and screening of subjects by the experimental technicians according to the inclusion and exclusion criteria; Subjects clean their faces with the designated cleansing sample, wipe the inner sides of their arms with dry paper, sit quietly in a laboratory with a temperature of $21 \pm 1^\circ\text{C}$ and a humidity of $50 \pm 10\%$ RH for 30 minutes; Mark the measurement area on the inner sides of the forearms, and the test area should be at least $3\text{ cm} \times 3\text{ cm}$ in size. The sample application area and the blank area should be randomly distributed within the marked area to ensure that the positions of the sample and the blank area are statistically balanced and that the intervals between the test areas are at least 1 cm; Modeling: After applying the sample area and the blank area with tape for about 20 times, causing visible redness to the naked eye; After modeling the inner sides of the subjects' arms, the test technicians use the skin data values before applying the sample by Tewameter to test the rate of water loss through the epidermis of the skin; The test technicians apply the sample evenly at a concentration of $(2.0 \pm 0.1)\text{ mg/cm}^2$ in the sample area and do not make any treatment in the blank area; Test the basic skin values of the subjects' faces: VISIA-CR image acquisition, VC20 image acquisition, Comeometer tests the moisture content of the stratum corneum of the skin, and Glossymeter tests the glossiness of the skin; Laboratory technicians guide the subjects to use the samples on-site according to the requirements for sample use and the application areas, and provide written test precautions and instructions. Test the arm skin data values of the subjects 15 minutes, 4 hours, 8 hours and 7 days after using the samples :Tewameter test for the transepidermal water loss rate of the skin; 2) Facial skin data values of the test subjects 15 minutes after using the samples :VISIA-CR image acquisition, VC20 image acquisition, Comcometer test for moisture content of the stratum corneum of the skin, Glossymeter test for skin gloss: The subjects filled out the self-assessment questionnaire [16-20].

2.10 Statistical analysis

All experimental data expressed as the mean \pm the standard deviation ($x \pm d$) values. ANOVA was used to analyze the experimental data, and Tukey's multiple comparison test was used to compare between the groups, with $P < 0.05$ considered to be statistically significant.

3. Results

3.1 HPLC analysis of TCE

The contents of 3 phenolic active ingredients in TCE were determined by the above analytical method. The HPLC chromatogram of the standard substance is shown in Figure 1A, and the HPLC chromatogram of the TCE sample is shown in Figure 1B. Calculated by the external standard method, in TCE, Gallic acid contains 1.78%, Chebulagic acid contains 17.80%, and Chebulinic acid contains 17.23%.

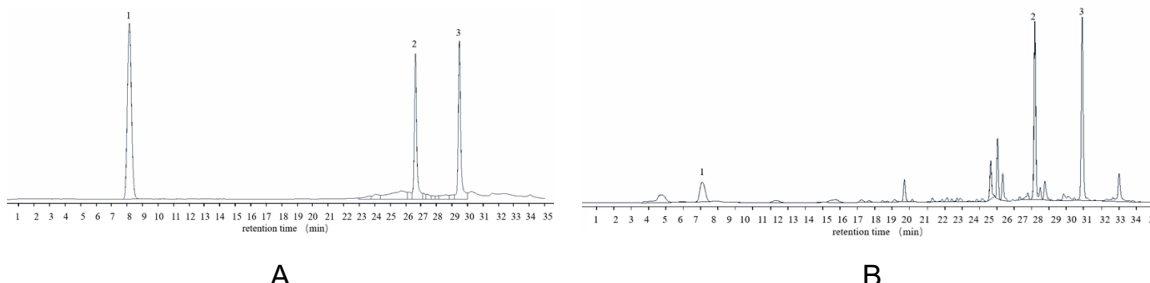


Figure 1. The HPLC chromatogram of the standard substance 1.gallic acid 2.chebulagic acid 3.chebulinic acid.(A) . The HPLC chromatogram of the TCE sample 1.gallic acid 2.chebulagic acid 3.chebulinic acid (B).

3.2 Network pharmacology and molecular docking of TCE

A total of 172 core small molecules and 172 potential anti-aging targets were predicted to overlap with 34 anti-aging targets in the self-owned database (Figure 2A), and 197 potential anti-inflammatory targets overlapped with 17 targets in the self-owned database (Figure 2B). The results of GO analysis of anti-aging targets (Figure 2C-F) and KEGG analysis of anti-aging targets (Figure 2F) showed that 37 aging targets were associated with 58 signaling pathways ($FDR < 0.05$). These 58 pathways are involved in the occurrence and development of aging. The figure describes 15 signaling pathways related to aging.

The GO analysis of anti-inflammatory targets(Figure 2G-I) and the KEGG analysis of anti-inflammatory targets (Figure 2J) showed that 17 anti-inflammatory targets were associated with 32 signaling pathways ($FDR < 0.05$). These 32 pathways are involved in the occurrence and development of inflammation. Sixteen inflammatory signaling pathways are described in the figure.

Based on the protein interaction network of 34 targets related to aging of core molecules, a PPI map was drawn (Figure 2K). According to the score ranking,6 core targets were selected (Figure 2M). Among the 6 core targets, the highest score ranking was AKT1 with a score of 50, followed by EGFR with a score of 39, and TP53 with a score of 37.

The PPI map was drawn based on the protein interaction network of 17 targets related to core molecules and inflammation (Figure 2L). Seven core targets were screened out according to the score ranking (Figure 2N). Among the seven core targets, the one with the highest score ranking was AKT1 with a score of 95, followed by TP53 with a score of 51, and EGFR with a score of 46.

The target AKT1 with the highest degree and existing in both aging and inflammation was selected for docking, and the docking energy results were shown in Table 1. Chebulinic acid has the lowest binding energy (-64.45 kcal/mol) , indicating that it has the strongest interaction with AKT1. Figure 2P shows the 3D structure diagram and 2D plane diagram of the docking of three small molecules with AKT1. The 2D structure diagram can be used to show the binding site and interaction force of small molecules with AKT1 receptor. Gallic acid interacted with Gln79, Asn54, Val270, and Trp80 amino acid residues of AKT1 receptor. Chebulinic acid interacted with AKT1 through Ser205, GLn203, Trp80, Asn53, Asn54, Val270, Arg273, and other amino acid residues. In addition, Chebulagic acid interacts with AKT1 through amino acid residues such as Asp274, Gly294, Gln79, Asp293 and Val270. The three small molecules interact with AKT1 mainly through hydrogen bonds^[5-6].

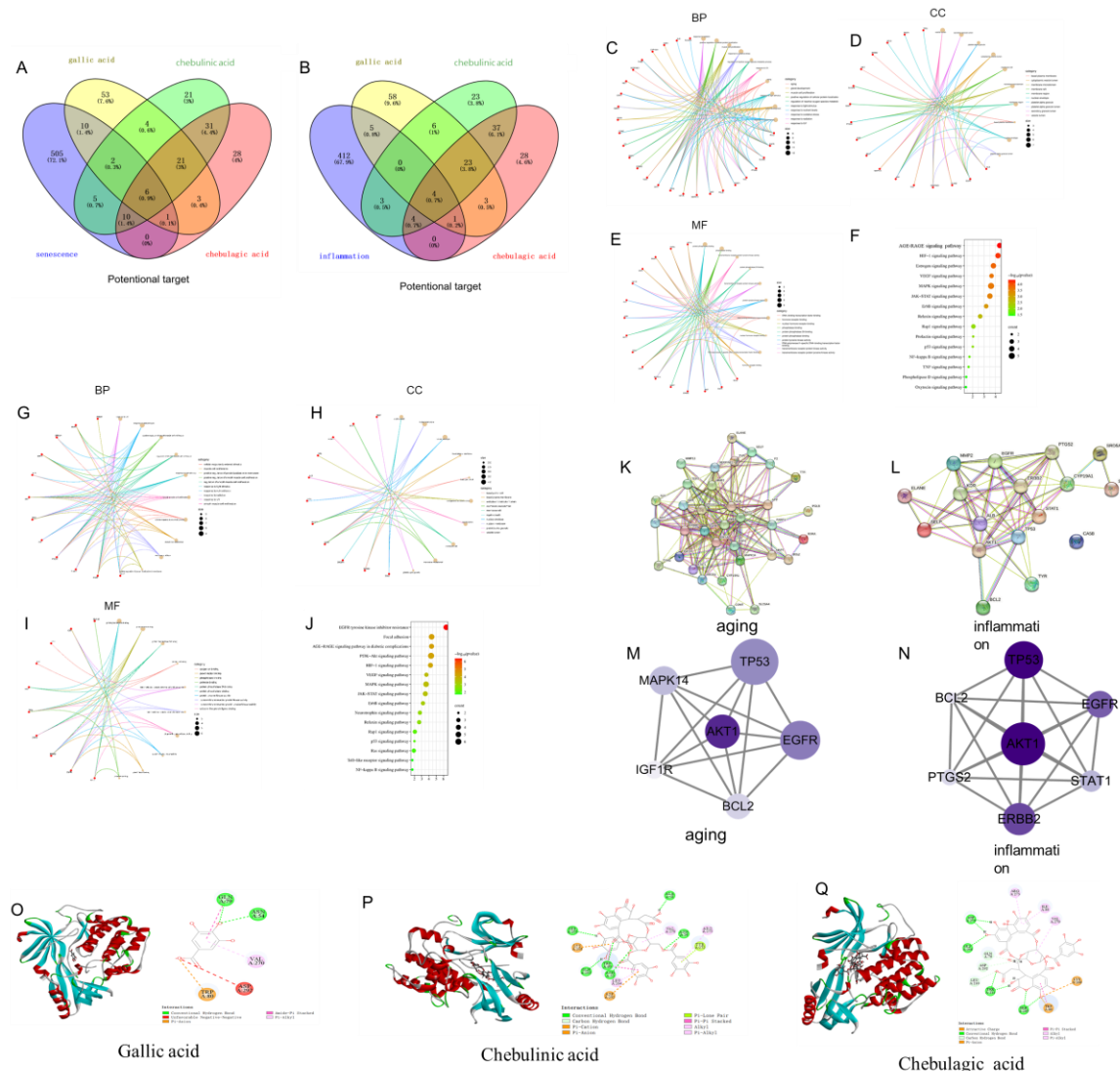


Figure 2. (A-B) Small Molecules and Free Database Aging(A) and Inflammation(B) Related Targets Venn diagram. (C-F) Anti-aging target GO function analysis cnetplot diagram, BP is a biological process (C), CC is a cell component (D), and MF is a molecular function (E). Analysis of anti-aging target KEGG signaling pathway (F). (G-J) Anti-inflammatory target GO function analysis cnetplot diagram; BP is a biological process (G), CC is a cell component (H), and MF is a molecular function (I). Analysis of anti-inflammatory target KEGG signaling pathway (J). (K-L) Protein-protein interaction diagram; (M-N) The core target obtained by cytoscape. (O-Q) Molecular docking of TCE three small molecules with AKT1 receptor 3D and 2D maps.

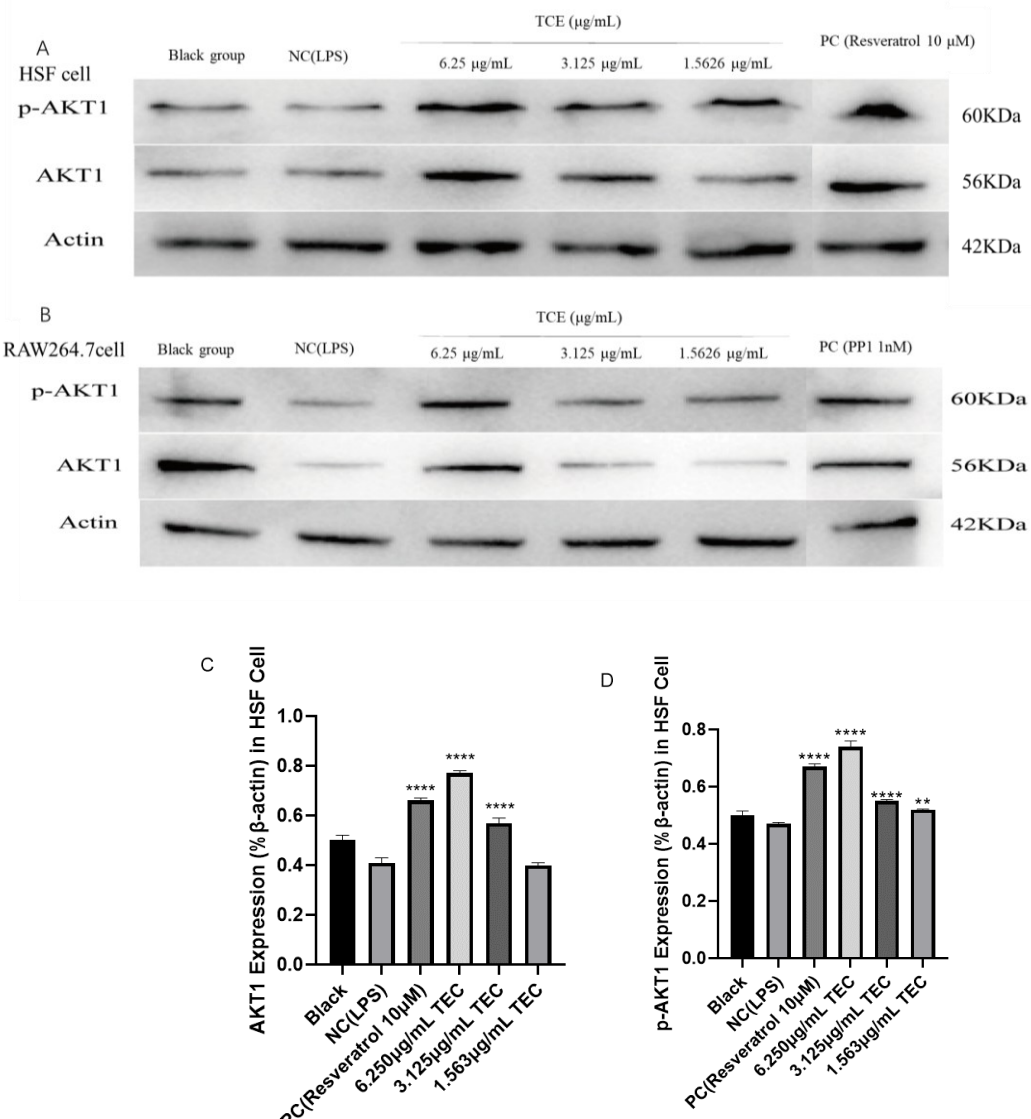
Table 1. The intermolecular docking energy (kcal/mol) of TCE core molecules

core molecules	docking energy (kcal/mol)
Gallic acid	-30.9991
Chebulinic acid	-64.4544
Chebulagic acid	-20.8492

3.3 Akt1 target validation

In HSF cells, the relative ratio of AKT1 protein expression in cells with 6.250 μ g/mL TCE to the negative control group was 1.88, significantly upregulated, and the relative ratio of p-AKT1 protein expression in cells to the negative control group was 1.81, significantly upregulated. The relative ratio of AKT1 protein expression in cells of 3.125 μ g/mL TCE to the negative control group was 1.38, significantly upregulated, and the relative ratio of p-AKT1 protein expression in cells to the negative control group was 1.18, significantly upregulated.

In RAW264.7, the relative ratio of AKT1 protein expression in cells with 12.500 μ g/mL TCE to the negative control group was 3.23, significantly upregulated, and the relative ratio of p-AKT1 protein expression in cells to the negative control group was 2.21, significantly upregulated. The relative ratio of AKT1 protein expression in cells of 6.250 μ g/mL TCE to that of the negative control group was 1.68, significantly upregulated, and the relative ratio of p-AKT1 protein expression in cells to that of the negative control group was 1.39, significantly upregulated. The relative ratio of AKT1 protein expression in cells of 3.125 μ g/mL TCE to that of the negative control group was 1.19, showing no significant difference. The relative ratio of p-AKT1 protein expression in cells to that of the negative control group was 1.42, significantly upregulated.



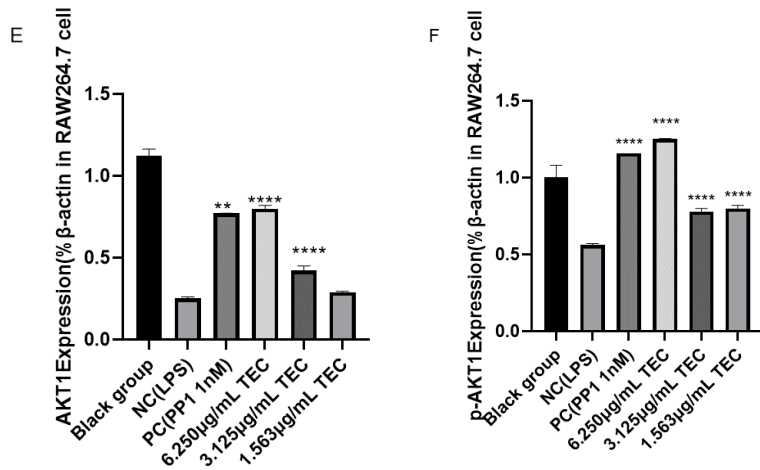


Figure 3. A Expression bands of AKT1 protein, p-AKT1 protein and β-ctin protein in HSF cells. B Expression bands of AKT1 protein, p-AKT1 protein and β-ctin protein in RAW264.7 cells. C The effect of TCE on the expression of AKT1 protein in HSF cells. D The effect of TCE on the expression of p-AKT1 protein in HSF cells. E The effect of TCE on the expression of AKT1 protein in RAW264.7 cells. F The effect of TCE on the expression of p-AKT1 protein in RAW264.7 cells. When conducting statistical analysis using the T-test method, Compared with the NC group, significance was expressed as *, P-value<0.05 was expressed as *, and P-value<0.01 was expressed as **, and P-value<0.0001 was expressed as ****.

3.4 Effects of TCE on Nrf2

Based on the 3D epidermal skin model (EpiKutis) immunofluorescence intensity images Figure 4A, the integrated optical density (IOD), whose value reflects the content of E2-related factor 2(Nrf2) Figure 4B.compared with the control group, the content of Nrf2 in the sample was significantly increased at a concentration of 0.1%(m/v), with an increase rate of 64.81%. This indicates that at this concentration, the content of nuclear factor E2-related factor 2(Nrf2) in the sample can be increased. It has antioxidant effects.

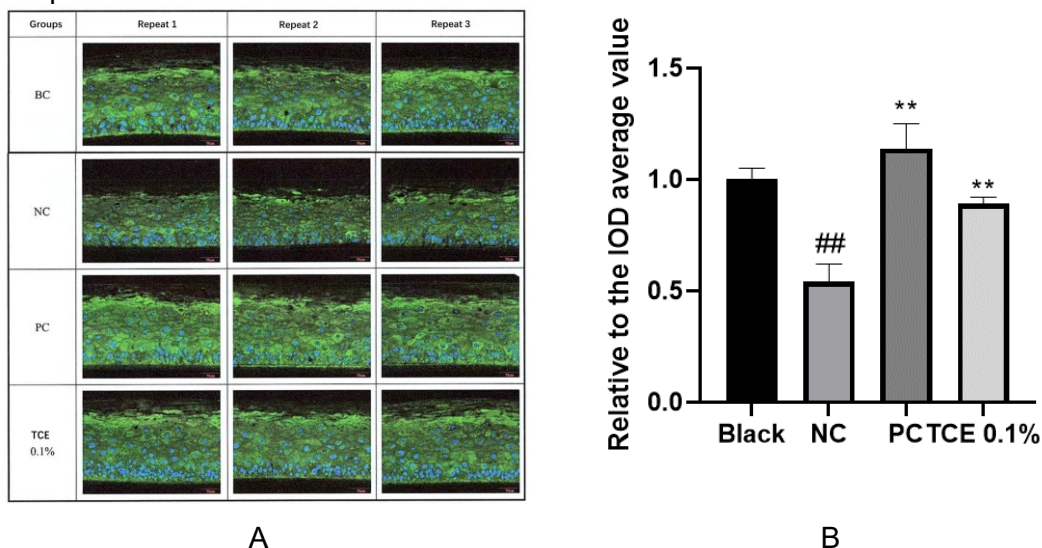


Figure 4. A:3D EpiKutis immunofluorescence intensity images. B: Bar chart of the relative integrated optical density (IOD) value of Nrf2. When conducting statistical analysis using the T-test method, compared with the BC group, significance was expressed as #, P-value<0.05 was expressed as #, and P-value<0.01 was expressed as ##. Compared with the NC group,

significance was expressed as *, P-value<0.05 was expressed as *, and P-value<0.01 was expressed as **.

3.5 The effect of TCE on TRPV1 in Hacat cells

Under the conditions of this experiment, the inhibition rates of TRPV1 of the sample TCE at concentrations of 0.078%, 0.039%, and 0.020% were $50.35\% \pm 1.65\%$, $34.76\% \pm 1.51\%$, and $21.05\% \pm 0.47$ respectively. Compared with the model group, P<0.05, showing a significant difference. It indicates that the TCE of this sample has the effect of inhibiting the expression of TRPV1 content at this concentration, and has anti-allergy and soothing effects.

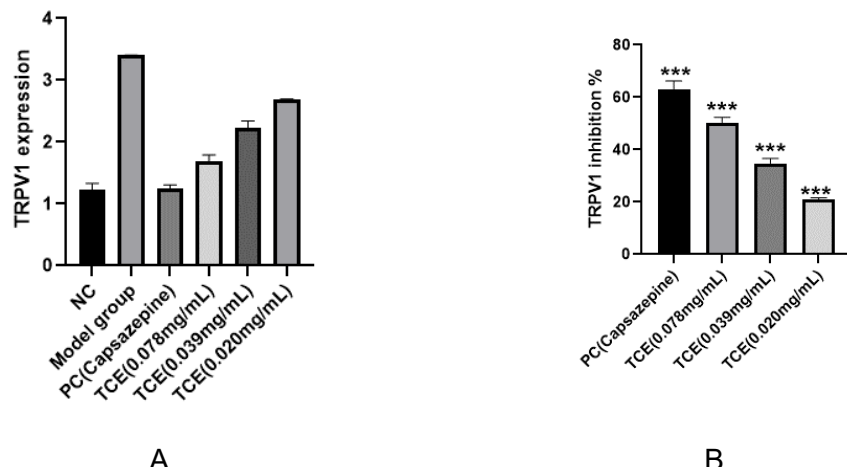
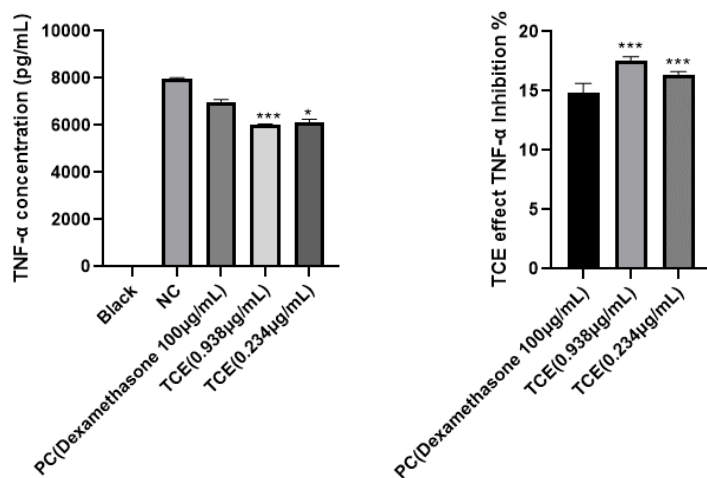


Figure 5. A: The expression level of TRPV1 in Hacat cells. B The inhibition rate of TRPV1 in Hacat cells by TCE. When conducting statistical analysis using the T-test method, Compared with the NC group, significance was expressed as *, P-value<0.05 was expressed as *, and P-value<0.01 was expressed as **, and P-value<0.001 was expressed as ***.

3.6 The effects of TCE on TNF- α in RAW264.7 cell

Under the action of concentrations of $0.938\mu\text{g}/\text{mL}$ and $0.234\mu\text{g}/\text{mL}$, the inhibition rates of TCE on the inflammatory factor TNF- α in RAW264.7 cell were 17.68% and 16.33% respectively, compared with the inhibition rate of PC the inhibition rate was statistically significant.



A**B**

Figure 6. A: The influence of TCE on the concentration of TNF- α . B: The inhibition of TCE on TNF- α in RAW264.7 cell. When conducting statistical analysis using the T-test method, Compared with the NC group, significance was expressed as *, P-value<0.05 was expressed as **, and P-value<0.01 was expressed as ***.

3.7 Clinical study

Compared with before use, after using the TCE-containing essence cream for 15 minutes, 4 hours, and 8 hours, the moisture content of the stratum corneum of the skin significantly increased ($P<0.05$), and the increase rates were 88.78%, 65.75%, and 43.41% respectively. After using the essence cream containing TCE for 7 days, 96.67% of the subjects agreed that their skin felt more moisturized compared to before use. Compared with before use, after using the essence cream containing TCE for 15 minutes, 4 hours and 8 hours, the transepidermal water loss rate of the skin was significantly reduced ($P<0.05$), and the reduction rates were 18.25%, 29.77% and 38.41% respectively. After 7 days of using the TCE-containing essence cream, 100% of the subjects agreed that there was a repairing effect after using the test sample, indicating that under this test condition, the TCE-containing essence cream has moisturizing and repairing effects.

Compared with before use, after using the TCE-containing essence cream for 15 minutes, 4 hours, 8 hours, and 7 days, the SEr value of the skin roughness parameter significantly increased ($P<0.05$), and the increase rates were 38.82%, 28.28%, 17.24%, and 25.33% respectively. After 7 days of using the essence cream containing TCE, 100% of the subjects agreed that there was a nourishing effect after using the test sample, indicating that under this experimental condition, the TCE-containing essence cream has nourishing effects.

Compared with before use, after using the essence cream containing TCE for 15 minutes, 4 hours, and 8 hours, the proportion of red area on the skin decreased significantly ($P<0.05$), and the reduction rates were 10.08%, 14.55%, and 18.43% respectively. After using the essence cream containing TCE for 7 days, 100% of the subjects agreed that they felt a significant skin soothing effect compared to before use. After using the TCE-containing essence cream for 7 days, 100% of the subjects agreed that their skin felt less tight compared to before use; after using the TCE-containing essence cream for 7 days, 100% of the subjects agreed that their skin felt no stinging compared to before use. After using the TCE-containing essence cream for 7 days, 100% of the subjects agreed that their skin did not become red compared to before use; after using the TCE-containing essence cream for 7 days, 100% of the subjects agreed that their skin did not become itchy compared to before use. After using the essence cream containing TCE for 7 days, 100% of the subjects agreed that their skin felt less hot compared to before use. After 7 days of using the TCE-containing essence cream, 100% of the subjects agreed that their skin felt more comfortable compared to before use, indicating that under the test conditions, the TCE-containing essence cream has a soothing effect [21-25].

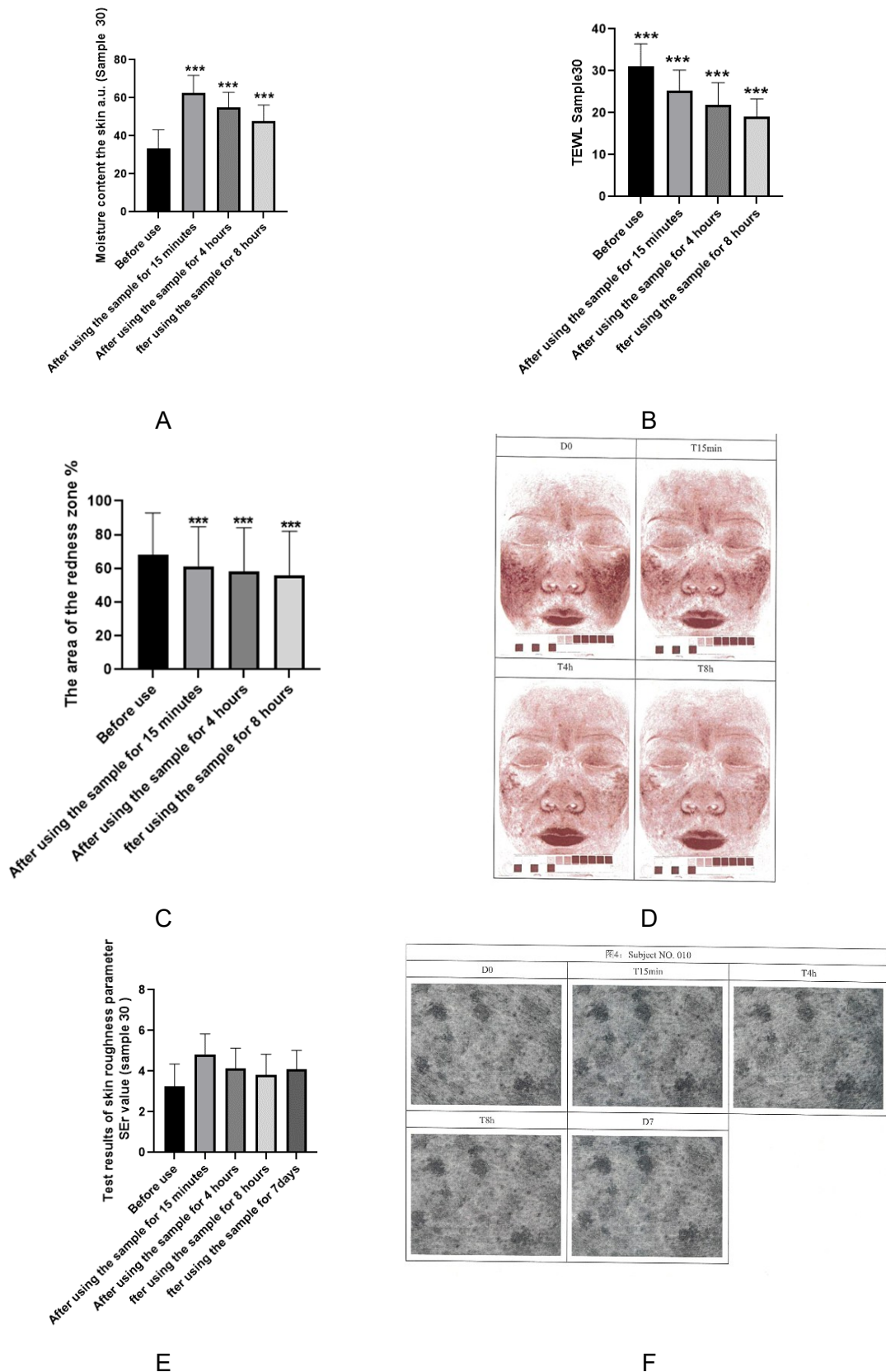


Figure 7. A: The moisture content of the stratum corneum of the skin after using the TCE-containing essence cream for 0 to 8 hours; B: The TEWL value of transdermal water loss of the skin within 0-8 hours after using TCE-containing essence cream. C: The proportion of red areas on the skin after using TCE-containing essence cream for 0-8 hours.D: Effective cases

of skin red area improvement are presented. E: The skin roughness value within 0 to 8 hours after using TCE-containing essence cream. F: Effective examples of skin roughness improvement are presented

When conducting statistical analysis using the T-test method, the visibility annotation method for the comparison chart of moisture content in the stratum corneum of the skin before and after using the sample, significance was expressed as *, P-value<0.05 was expressed as *, and P-value<0.01 was expressed as **, and P-value<0.001 was expressed as ***

4. Discussion

The method of network pharmacology and molecular docking to calculate the biological targets, which expanded the idea for the development of natural plants. According to the results of computational chemistry, several dimensions of anti-aging of sensitive skin were verified, and the results were consistent with expectations. In addition, we found the connection between AKT1 and the TRPV, Inflammation family, and this pathway is expected to be validated by the model of inflammation and aging for sensitive skin, which will guide our future research direction.

5. Conclusion

Our research results indicate that TCE plays an important role in the inflammatory aging process in the skin by specifically targeting the AKT1-mediated signaling pathway. We utilized network pharmacology to accurately predict the potential regulatory targets of the core component of nuclear TCE, thereby studying its potential ability to precisely act on anti-aging and anti-inflammatory targets^[26-27]. The core target AKT1 was found through the molecular docking between the core key small molecule component (ligand) of TCE and the target (receptor). The effect of khobutin on AKT1 protein in macrophages and fibroblasts during inflammatory responses was explored through in vitro cell model experiments to verify the potential mechanism of its anti-inflammatory effect. The correlation between AKT1 and the inflammatory pathway was confirmed by verifying the effect of TCE on the typical inflammatory factor TNF- α . Nrf2, as a key molecule for cells to resist oxidative stress, plays an important role in maintaining the REDOX balance of cells and is closely related to skin aging^[28-29]. The excellent performance of Nrf2 on the skin in vitro was observed through TCE. The above verification experiments show. AKT1 is known to be involved in regulating various metabolic states and cell proliferation stages^[30]. The data of this study suggest that the multiple activities of Cheburokhov in the skin aging pathways caused by UV-induced oxidation and inflammation may be related to its regulation of AKT1. In human data, Terminalia Chebula demonstrated immediate relief of facial redness and long-term reduction of skin roughness, which is consistent with in vitro experiments for alleviating inflammatory aging. A detailed study on the molecular mechanism of Chekhov in inflammatory aging will be further clarified in the subsequent work.

Reference

- [1] Chulasiri M, Wanaswas P, Sriaum D, et al. Utilizing hydroglycolic extract from myrobalan fruits to counteract reactive oxygen species[J]. International journal of cosmetic science, 2011, 33(4): 371-376.
- [2] Saha S, Verma R J. Antioxidant activity of polyphenolic extract of Terminalia chebula Retzius fruits[J]. Journal of taibah university for science, 2016, 10(6): 805-812.

- [3] Du L Y, Li G, Jiang T, et al. Network pharmacology integrated molecular docking reveals the bioactive components and potential targets of ginseng anti-skin ageing mechanism[J]. 2021.
- [4] SHANNON P, MARKIEL A, OZIER O, et al. Cytoscape: a software environment for integrated models of biomolecular interaction networks [J]. Genome Research, 2003, 13(11): 2498-2504.
- [5] Liu Y, Yang X, Gan J, et al. Improved protein-ligand blind docking by integrating cavity detection, docking and homologous template fitting., 2022, 50, pp[J]. W159-W164.
- [6] Yang X, Liu Y, Gan J, et al. FitDock: protein-ligand docking by template fitting[J]. Briefings in Bioinformatics, 2022, 23(3): bbac087.
- [7] Bai X, Tang Y, Li Q, et al. Network pharmacology integrated molecular docking reveals the bioactive components and potential targets of *Morinda officinalis*-*Lycium barbarum* coupled-herbs against oligoasthenozoospermia. Sci Rep. 2021; 11 (1): 2220.
- [8] Grossman B J , Shanley T P , Denenberg A G ,et al.Phosphatase inhibition leads to activation of I κ B kinase in murine macrophages[J].Biochemical & Biophysical Research Communications, 2002, 297(5):1264-1269.
- [9] Somanath P R, Chen J, Byzova T V. Akt1 is necessary for the vascular maturation and angiogenesis during cutaneous wound healing[J]. Angiogenesis, 2008, 11: 277-288.
- [10] Eto R, Abe M, Hayakawa N, et al. Age-related changes of calcineurin and Akt1/protein kinase B α (Akt1/PKB α) immunoreactivity in the mouse hippocampal CA1 sector: an immunohistochemical study[J]. Metabolic brain disease, 2008, 23: 399-409.
- [11] Maher J M , Dieter M Z , Aleksunes L M ,et al.Oxidative and electrophilic stress induces multidrug resistance-associated protein transporters via the nuclear factor-E2-related factor-2 transcriptional pathway.[J].Hepatology, 2010, 46(5).
- [12] Gunthorpe M J , Chizh B A .Clinical development of TRPV1 antagonists: targeting a pivotal point in the pain pathway.[J].Drug Discovery Today, 2009, 14(1-2):56-67.DOI:10.1016/j.drudis.2008.11.005.
- [13] Coecke,S Balla,M Bowe,G, Guidance on good cell culture practice, A report of the second ECVAM task force on good cell practice,2005.
- [14] TSHRH 034-2021 Cosmetic soothing effect test - In vitro determination of TNF- α inflammatory factor content - Lipopolysaccharide-induced macrophage RAW264.7 test method.China.
- [15] Ava Rhule , Severine Navarro , Jerry R. Smith ,Panax notoginseng attenuates LPS-induced pro-inflammatory mediators in RAW264.7 cells. Journal of Ethnopharmacology 106 (2006) 121–128.
- [16] Fluhr JW, Pfisterer S,Gloor M, Direct Comparison of Skin Physiology in Children and Adults with Bioengineering Method [J], Pediatric Dermatology,2010,17;436-439.
- [17] Lim SH,Kim SM,Lee yW, et al, Change of biophysical properties of the skin caused by ultraviolet radiation-induced photodamage in Koreans , Skin Res Technol,2010,14(1);93-102
- [18] Sadhra SS,Kurmi OP, Mohammed NI,et al, Protection afforded by controlled application of a barrier cream :a study in a workplace setting [J], Br J Dermatol, 2014,171(4) ;813-818.
- [19] Shyr T,Ou-Yang H, Sunserien formulations may serve as additional water barrier on skinsurface:a clinical assessment [J], Int J Cosmet Sci. 2016,38(2):164-169.
- [20] Marty Visscher, Vivek Narendran, Imaging reveals distinct textures at three infant skinsites and reflects skin barrier status, Skin Res Technol,2021,27(2) 145-152.
- [21] Qin O,Tan YM,Jiang WC,et al, Non-invasive assessment of changes and repair dynamics post irritant intervention in skin barrier [J]. Int J Clin Exp Med,2018,11(5),4490-4499.
- [22] Gao YR,Wang XM,Chen SY,et al, Acute skin barrier disruption with repeated tape stripping:An in vivo model for damage skin barrier [J]. Skin Res Technol,2012,19(2):162;168.

- [23] Konya C, Sanada H, Sugama J, et al. Skin injuries caused by medical adhesive tape in older people and associated factors[J]. Journal of Clinical Nursing, 2010, 19(9-10):1236-1242.
- [24] Tokumura F, Umekage K, Sado M, et al. Skin irritation due to repetitive application of adhesive tape: the influence of adhesive strength and seasonal variability [J]. Skin Res Technol, 2005, 11(2):102-106.
- [25] Perugini P, Vettor M, Rona C, et al. Efficacy of oleuropein against UVB irradiation: preliminary evaluation[J]. Int J Cosmet Sci, 2010, 30(2):113-120.
- [26] Lee Y, Byun H S, Seok J H, et al. Terminalia Chebula provides protection against dual modes of necroptotic and apoptotic cell death upon death receptor ligation[J]. Scientific reports, 2016, 6(1): 25094.
- [27] Das G, Kim D Y, Fan C, et al. Plants of the genus Terminalia: An insight on its biological potentials, pre-clinical and clinical studies[J]. Frontiers in Pharmacology, 2020, 11: 561248.
- [28] John, D, Hayes, et al. The Nrf2 regulatory network provides an interface between redox and intermediary metabolism[J]. Trends in Biochemical Sciences, 2014, 39(4):199-218.
- [29] Sykotis G P, Bohmann D. Stress-Activated Cap'n'collar Transcription Factors in Aging and Human Disease[J]. Science Signaling, 2010, 3(112).
- [30] Naeem A S. The role of Akt1 in skin barrier formation[D]. UCL (University College London), 2014.